
ROBUST MULTIMODAL LEARNING WITH MISSING MODALITIES VIA PARAMETER-EFFICIENT ADAPTATION

Md Kaykobad Reza¹, Ashley Prater-Bennette², M. Salman Asif¹

¹ University of California Riverside, CA 92508, USA

² Air Force Research Laboratory, Rome, NY 13441, USA

mreza025@ucr.edu, ashley.prater-bennette@us.af.mil, sasif@ucr.edu

ABSTRACT

Multimodal learning seeks to utilize data from multiple sources to improve the overall performance of downstream tasks. It is desirable for redundancies in the data to make multimodal systems robust to missing or corrupted observations in some correlated modalities. However, we observe that the performance of several existing multimodal networks significantly deteriorates if one or multiple modalities are absent at test time. To enable robustness to missing modalities, we propose simple and parameter-efficient adaptation procedures for pretrained multimodal networks. In particular, we exploit low-rank adaptation and modulation of intermediate features to compensate for the missing modalities. We demonstrate that such adaptation can partially bridge performance drop due to missing modalities and outperform independent, dedicated networks trained for the available modality combinations in some cases. The proposed adaptation requires extremely small number of parameters (e.g., fewer than 0.7% of the total parameters in most experiments). We conduct a series of experiments to highlight the robustness of our proposed method using diverse datasets for RGB-thermal and RGB-Depth semantic segmentation, multimodal material segmentation, and multimodal sentiment analysis tasks. Our proposed method demonstrates versatility across various tasks and datasets, and outperforms existing methods for robust multimodal learning with missing modalities.

1 Introduction

Multimodal learning (MML) [4, 51] is a general framework for processing, combining, and understanding information from multiple, diverse data sources. Fusing knowledge from multiple modalities (e.g., text, images, audio, and sensor data) is expected to provide more accurate and reliable systems. In recent years, MML has achieved remarkable success in a wide range of applications, including image segmentation [6, 44, 56], captioning [53, 57], classification [12, 35], sentiment analysis [23, 39], and autonomous driving [34, 49]. In all these applications, one often encounters situations where some modalities are corrupted or missing due to hardware limitations/failures or data acquisition cost/constraints. The ability to handle corrupt or missing modalities is thus crucial for the robustness and reliability of multimodal systems. The central question of this paper is to study and build robustness in MML with missing modalities.

Recent studies [15, 30, 32] have shown that MML is not inherently robust to missing modalities and performance can drop significantly when modalities are missing at test time. Existing approaches for robust MML usually work for specific combinations of modalities they are trained for and tend to perform poorly when applied to untrained combinations. For instance, one approach is to adopt robust training strategies such as modality dropout during training [20, 33], partial or full modality masking [2, 37], and knowledge distillation [31, 41]. These approaches either require specialized training strategies or utilize extra models/sub-networks to guide the underlying model. Another approach replaces uninformative tokens with aggregated informative tokens from different modalities or learns to predict tokens for the specific missing modalities [37, 44, 47]. Training such separate (independent) networks for every possible modality combination is not feasible. One recent approach for robust MML is to impute missing modalities from the available modalities [9, 36, 52]. Performance of these methods depend on the generation model that imputes the missing modalities.

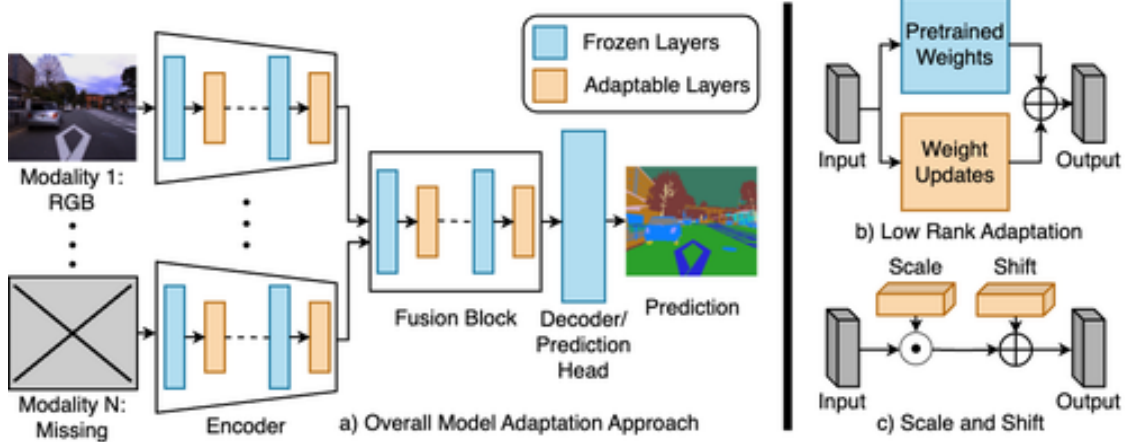


Figure 1: a) Overview of our approach for robust multimodal learning with missing modalities via parameter-efficient adaptation. A model pretrained on all the modalities is adapted using a small number of parameters to handle different modality combinations. b) Low-rank model adaption computes features using frozen and low-rank weights and combine them. c) Scale and shift feature adaptation transforms input by element-wise multiplication and addition. One set of parameters is learned for each modality combination.

In this paper, we propose a parameter-efficient approach to build a multimodal network that can adapt to arbitrary combinations of input modalities. Our main objective is to modify the network in a controllable manner as a function of available modalities. Figure 1 illustrates our proposed method, where a given multimodal network can be adapted to arbitrary modality combinations by transforming the intermediate features at different layers. To achieve parameter-efficient adaptation, we propose to use simple linear transformations such as scaling, shifting, or low-rank increments of features. Our method does not require retraining the entire model or any specialized training strategy. The adapted networks provide significant performance improvement over the multimodal networks trained with all modalities and tested with missing modalities. Performance of the adapted models is also comparable or better than the models that are exclusively trained for each input modality combination. We present a series of experiments to evaluate our method and compare with existing methods for robust MML. We tested different parameter-efficient adaptation strategies and found scaling and shifting features provides overall best performance with less than 0.7% of the total parameters.

Contributions. The main contributions can be summarized as follows.

- We propose parameter-efficient adaptation for multimodal learning that is robust to missing modalities. The adapted model can easily switch to different network states based on the available modalities with minimal latency, computational, or memory overhead.
- The adapted networks provide notably improved performance with missing modalities when compared to models trained with all modalities and is comparable to or better than the networks trained for specific modality combinations.
- Our approach is versatile and adaptable to a wide range of multimodal tasks and models. Detailed evaluations on diverse datasets and tasks show that our approach outperforms existing baseline methods and robust models designed for specific tasks and datasets.

2 Related Work

Multimodal learning with missing modalities has been studied for different applications in recent years. For instance, robustness in vision-language tasks with multimodal transformers in [30], multimodal sentiment analysis in [32], multimodal classification in [15], and multimodal action recognition in [47]. These studies have shown that the task performance can drop significantly when modalities are missing during test time.

Robust training strategies have been proposed to make models robust to different missing modalities. Such approaches include modality dropout during training [20, 33], unified representation learning [24], and supervised contrastive learning [11]. Modality masking during training has become a popular choice for enhancing robustness. [37] utilized complementary random masking, [17] used masked auto encoder, and [30] applied masked cross-modal attention for enhancing robustness of the underlying model. [15] proposed noisy perturbation of modalities during training for robust multimodal sentiment analysis.

Design of robust models and fusion strategies is another approach for robust MML. [10] proposed a recursive meshing technique called SpiderMesh and [37] designed complementary random masking and knowledge distillation based framework for robust RGB-thermal semantic segmentation. [44] proposed TokenFusion to dynamically detect and replace uninformative tokens with projected tokens from other modalities for robust RGB-depth semantic segmentation, image-to-image translation, and 3D object detection. [43] proposed a model that learns modality-shared and modality-specific features for robust brain tumour segmentation. [7] proposed a robust fusion strategy for multimodal classification. The main limitation of these methods is that they are generally designed for a specific modality combination and do not perform well when applied to other multimodal tasks [27].

Knowledge distillation and generation methods have also become popular for robust MML. Studies by [36] and [52] used GAN based generative models while [9] used VAE based generative models for imputing missing modalities from available input modalities for underlying multimodal tasks. Different knowledge distillation approaches have also been applied in several multimodal tasks. [41] proposed mean teacher and [31] introduced multimodal teacher for semi-supervised image segmentation. [37] and [15] applied self-distillation loss for robust RGB-thermal semantic segmentation. Apart from these approaches, weight space ensembling [48], policy learning [30] and optimal fusion strategy designing [31] were also studied for robust MML for various tasks.

3 Proposed Method

3.1 Adaptation for Missing Modalities

Let us denote the set of input modalities for a given task as $\mathcal{M} = \{m_1, \dots, m_M\}$. Given the full set \mathcal{M} , one can train a model f with parameters $\Theta_{\mathcal{M}}$ that maps inputs for all the modalities (denoted as $\mathcal{X}_{\mathcal{M}}$) to an output $y_{\mathcal{M}}$ as

$$y_{\mathcal{M}} = f(\mathcal{X}_{\mathcal{M}}; \Theta_{\mathcal{M}}). \quad (1)$$

If a subset of the modalities \mathcal{M} is missing, a naïve approach is to train a new model for the available input modalities. Without loss of generality, suppose $\mathcal{K} \subset \mathcal{M}$ represents missing modalities. We can use $\mathcal{S} = \mathcal{M} \setminus \mathcal{K}$ modalities to retrain the model f for a new set of parameters $\Theta_{\mathcal{S}}$ as

$$y_{\mathcal{S}} = f(\mathcal{X}_{\mathcal{S}}; \Theta_{\mathcal{S}}), \quad (2)$$

where $\mathcal{X}_{\mathcal{S}}$ represents input data for modalities in \mathcal{S} . While we would prefer that $y_{\mathcal{S}} \approx y_{\mathcal{M}}$, but the training above does not guarantee it. In principle, we can train one model for every possible $\mathcal{S} \subset \mathcal{M}$ and use the corresponding model at the test time. Such an approach is infeasible because of computational and storage resources required to train models for a large number of possible modality combinations. Furthermore, deploying a large number of trained models and selecting one of them at test time is not feasible in real-world scenarios.

We propose an alternative approach to adapt a single model for all $\mathcal{S} \subset \mathcal{M}$ in a parameter-efficient manner. In particular, we train the model f on the full set of modalities \mathcal{M} and freeze the parameters $\Theta_{\mathcal{M}}$. We add a small number of parameters $\Delta_{\mathcal{S}}$, corresponding to the available modality set \mathcal{S} , and update the model as

$$\hat{y}_{\mathcal{S}} = f(\mathcal{X}_{\mathcal{S}}; \Theta_{\mathcal{M}}, \Delta_{\mathcal{S}}) \quad (3)$$

such that $\hat{y}_{\mathcal{S}} \approx y_{\mathcal{S}}$ in the worst case and $\hat{y}_{\mathcal{S}} \approx y_{\mathcal{M}}$ in the best case. Such an adaptation is parameter-efficient if the number of parameters in $\Delta_{\mathcal{S}}$ is significantly smaller than that in $\Theta_{\mathcal{M}}$. In our experiments, we keep $\Theta_{\mathcal{M}}$ frozen and demonstrate that less than 0.7% of the total parameters for $\Delta_{\mathcal{S}}$ are sufficient for network adaptation.

3.2 Methods for Adaptation

In recent years, a number of parameter-efficient methods have been proposed for network adaptation for various tasks. To the best of our knowledge, none of them have been applied for multimodal adaptation to handle missing modalities. In this section, we discuss some of the methods that we used to build our proposed adaptation method for robust MML with missing modalities.

Low-rank adaptation (LoRA) is one possible way to adapt models to missing modality scenarios. Such adaptation has been applied in other domains and tasks. For instance, LoRA in transformers [19] and KAdaptation [18] learn low-rank factors for task/domain adaptation. In our context, suppose W represents one of the weight matrices in the pretrained $\Theta_{\mathcal{M}}$. For a given \mathcal{S} , we can learn a low-rank matrix $W_{\mathcal{S}}$ for $\Delta_{\mathcal{S}}$. Since the update matrix is low-rank, the number of parameters needed for $\Delta_{\mathcal{S}}$ remains a fraction of that in $\Theta_{\mathcal{S}}$.

Scaling and shifting features (SSF) is another parameter-efficient method to transform intermediate features of the pretrained model [25, 21]. As shown in Figure 1c, SSF applies a linear transformation to the given token/feature with learnable scale (γ) and shift parameters (β). Given an input token x , SSF generates the output token h as

$h = \gamma \odot x + \beta$, where γ, β, x, h are vectors of same length and \odot represents element-wise multiplication along the embedding dimension. These scale and shift parameters are input-independent, meaning they are applied to the features regardless of the specific input modality. They are learned during the training process to help the model adjust and fine-tune its representations for better performance on the underlying task.

BitFit in [5] and **Norm** adaptation (both batch norm and layer norm) are other approaches that adapt a subset of the model parameters. BitFit adapts the bias terms and Norm adaptation adapts norm layers, while keeping everything else frozen. Our experiments show that intermediate feature modulation via these simple linear transformation works well for most of the scenarios.

3.3 Our Approach: Parameter-Efficient Adaptation for Missing Modalities

Our overall approach for model adaptation is illustrated in Figure 1. We first train a network with all available modalities in \mathcal{M} and freeze the weights $\Theta_{\mathcal{M}}$. To adapt the model for different $\mathcal{S} \subset \mathcal{M}$, we insert SSF layers after each linear, convolutional, and norm (both batch norm and layer norm) layers. We learn (γ, β) for all the SSF layers for given \mathcal{S} . While training SSF parameters for the given modality combination, \mathcal{S} , we set the missing modalities to zero. At the test time, we can easily change the SSF parameters corresponding to the available modalities. We only insert SSF layers in the encoder and fusion blocks, while keeping the decoder/prediction head unchanged. We observed that using pretrained decoder/prediction head provided a good overall performance with several missing modalities.

We primarily selected the SSF technique for robust multimodal learning with missing modalities because of its simplicity and effectiveness. SSF was introduced in [21] with batch normalization to potentially enhance the representation power of the networks and faster convergence. [1] used the same strategy for layer normalization and [25] used it for fine-tuning pretrained models for different image classification tasks on several datasets. SSF offers several benefits: First, the parameters (γ, β) are independent of the input features, which makes SSF applicable to diverse tasks and input modality combinations. Second, we can easily insert SSF layers in the existing model without changing the model architecture. We can easily switch/select the corresponding SSF parameters for a given input modality combination. Finally, SSF introduces extremely small number of additional learnable parameters. The resulting adaptation offers significant savings compared to training a separate model for each input combination or retraining the model using some specialized training strategy like modality dropout or knowledge distillation.

4 Experiments and Results

We performed detailed experiments to evaluate the performance of our proposed method for different tasks and datasets. We also present comparison with existing methods that are robust to missing modalities.

4.1 Datasets

Multimodal segmentation. We used three datasets for three multimodal segmentation tasks. MFNet with RGB-Thermal images [14], NYUDv2 with RGB-Depth images [38] and MCubeS for multimodal material segmentation with RGB, Angle of Linear Polarization (AoLP), Degree of Linear Polarization (DoLP) and Near-Infrared (NIR) images [26]. These datasets are divided into train and test sets along with ground truth per-pixel annotation for the underlying segmentation tasks.

Multimodal sentiment analysis. CMU-MOSI from [55] and CMU-MOSEI from [3] are two popular datasets for multimodal sentiment analysis using audio, visual and text as input modalities. They contain 2199 and 23453 annotated data samples, respectively, divided into train, validation, and test sets.

4.2 Implementation Details

To investigate missing modality adaptation performance in multimodal semantic and material segmentation tasks, we use the CMNeXt model [56] as the base model. We use multimodal transformer [42] as the base model for multimodal sentiment analysis. We train a base model with all the modalities for each dataset. To evaluate performance with missing modalities, we provide the available modalities and set the missing modalities to zero. To perform model adaptation for any modality subset $\mathcal{S} \subset \mathcal{M}$, we freeze the pretrained weights and insert learnable SSF layers. Then we fine tune the learnable parameters for 100 epochs for multimodal segmentation tasks and until convergence for multimodal sentiment analysis tasks.

For multimodal segmentation tasks, we set the initial learning rate to 6×10^{-5} and applied a polynomial learning rate scheduler with a power of 0.9. The first 10 epochs were set as the warm-up, during which the learning rate was set to 0.1 times the original rate. The scale parameters (γ) were initialized with all 1s and the shift parameters (β) were

Table 1: Performance of Pretrained, Dedicated, and Adapted networks with missing modalities. CMNeXt is the base model for multimodal semantic segmentation for MFNet and NYUDv2 datasets and multimodal material segmentation for MCubeS dataset. HHA-encoded images were used instead of raw depth maps. **Bold** letters represent best results.

Dataset	Input	Missing	Pretrained	Dedicated	Adapted
MFNet	RGB-Thermal	-	60.10	60.10	-
	RGB	Thermal	53.71	55.86	55.22
	Thermal	RGB	35.48	53.34	50.89
NYUDv2	RGB-Depth	-	56.30	56.30	-
	RGB	Depth	51.19	52.18	52.82
	Depth	RGB	5.26	33.49	36.72
MCubeS	RGB-AoLP-DoLP-NIR	-	51.54	51.54	-
	RGB-AoLP-DoLP	NIR	49.06	49.48	51.11
	RGB-AoLP	DoLP-NIR	48.81	48.42	50.62
	RGB	AoLP-DoLP-NIR	42.32	48.16	50.43

initialized with all 0s. We used cross-entropy loss function and AdamW optimizer as proposed in [29], with an epsilon value of 10^{-8} and a weight decay of 0.01. We used a batch size of 4 and report single scale performance for all the datasets. All other hyper-parameters and configurations are the same as [56]. For multimodal sentiment analysis tasks, we used the default settings for the datasets as configured in the codebase [54]. We have included additional details for each dataset and experimental setup in the supplementary section.

4.3 Baseline Methods

We report experiments and results for different methods that are listed as follows. **Pretrained** model refers to the base model that is trained with all the available modalities. **Dedicated** training refers to independent models trained for each input modality combination. **Adapted** model refers to the model that is adapted using our approach for each input modality combination.

Different robust methods have been proposed for different multimodal tasks. We compare our method with the following methods: SpiderMesh [10], VPFNet [27], MDRNet [58], CRM [37] for robust RGB-thermal semantic segmentation. CEN [45], TokenFusion [44], AsymFusion [46], Dilated FCN-2s [22] for robust RGB-depth semantic segmentation.

For every task/dataset, we adopted the experimental setup used in the corresponding previous studies. We used the reported results from prior works where possible. It is important to note that, because of this criteria, some of the baseline methods may only be present in specific experiments depending on the availability of their reported numbers. We also perform detailed comparison analysis of SSF with other parameter-efficient adaptation techniques. For all the experiments we follow the same setup suggested by the corresponding papers and report mean accuracy, F1 score and mean intersection over union (mIoU) when available.

Ablation studies and comparison of different parameter-efficient adaptation methods show that SSF-based adaptation provides overall best performance. We present results for scale only, shift only, BitFit [5], norm layer fine-tuning and LoRA [19].

4.4 Experiments for Multimodal Segmentation

In this section, we present experiments for multimodal semantic segmentation with RGB-Thermal and RGB-Depth datasets, and multimodal material segmentation with MCubeS dataset. We report the detailed results for multimodal material segmentation along with per class % intersection over union (IoU) comparisons between the Pretrained and Adapted models in the supplementary section.

Overall performance comparison. We present the performance comparison of Pretrained, Dedicated, and Adapted networks for different missing modalities in Table 1. We observe that the performance of the Pretrained model drops significantly with missing modalities. We see a 6.39% drop when Thermal is missing in MFNet dataset and 5.11% drop when Depth is missing in NYUDv2 dataset compared to the case when all modalities are available. The effect is amplified when RGB gets missing as we observe 24.62% drop in MFNet dataset and 51.04% drop in NYUDv2

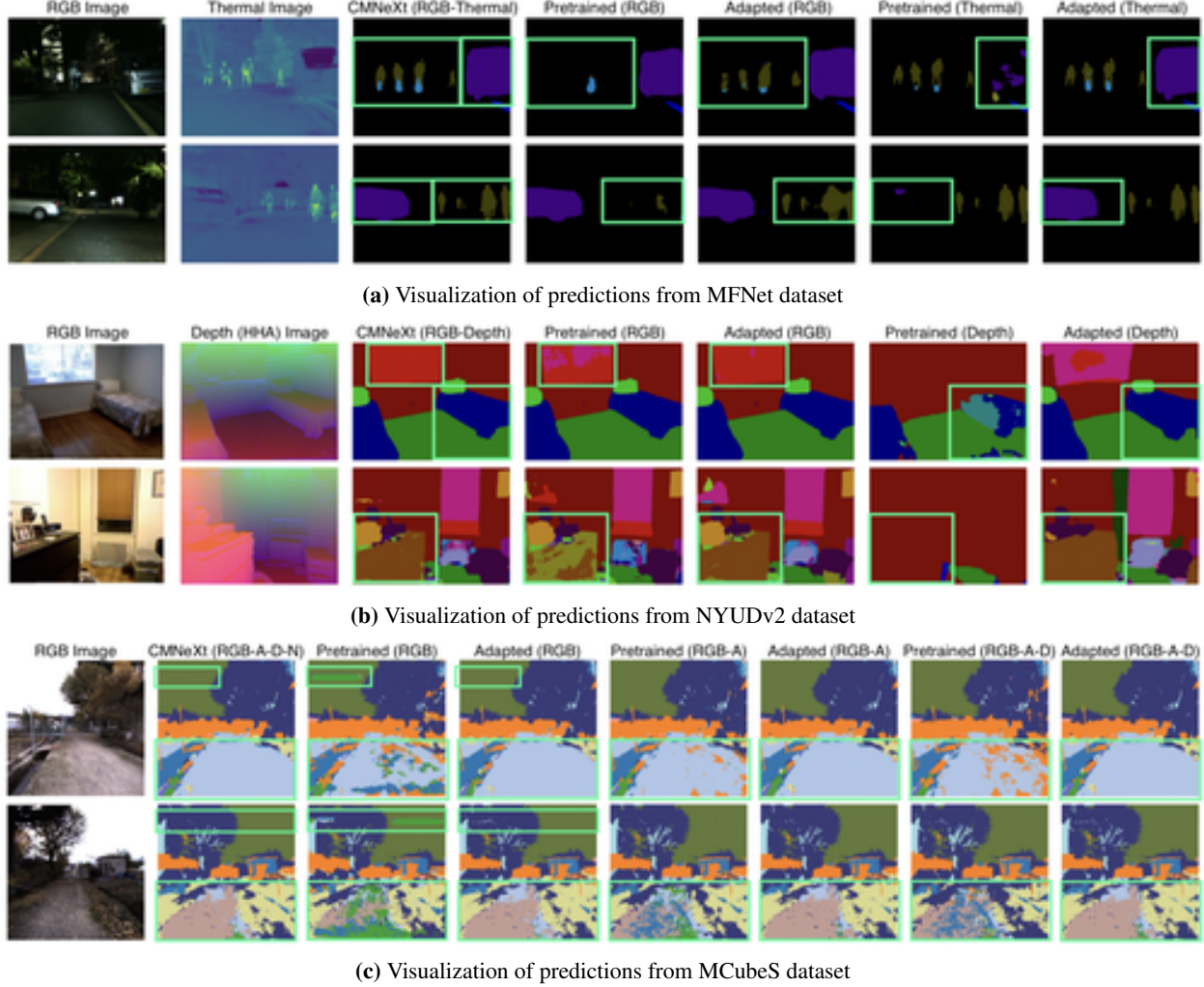


Figure 2: Examples of predicted segmentation maps for the Pretrained and Adapted models for multimodal semantic segmentation (on MFNet and NYUDv2) and material segmentation (on MCubeS). Title above each subimage shows method name (tested with available modalities). CMNeXt column shows the predictions with all the modalities. Segmentation quality improves significantly after model adaptation for all the input modality combinations. Green boxes highlight areas with salient differences in results (e.g., cars and humans missing in the Pretrained model with missing modalities but visible in the Adapted model). For MCubeS dataset, we only show RGB images and A, D and N denote angle of linear polarization, degree of linear polarization, and near-infrared, respectively.

dataset. In MCubeS dataset, we observe 2.48–9.22% drop in pretrained model when different modality combinations are missing.

The overall performance of Adapted models with missing modalities is significantly better than Pretrained models. For MFNet, an improvement of 1.51% compared to the Pretrained model when RGB is available and thermal is missing. The Adapted model performance is close to the performance of Dedicated network trained for RGB only. The adapted model shows a significant improvement of 15.41% compared to the Pretrained model when RGB is missing. For NYUDv2 dataset, we see 1.63% and 31.46% performance improvement compared to Pretrained model when depth and RGB are missing, respectively. In both cases, the performance of the Adapted model is better than the Dedicated model. For all input combinations in MCubeS dataset, we see 1.82–8.11% performance improvement compared to the Pretrained model. The Adapted model performs better than Dedicated models in all the cases.

Visualization of segmentation maps. For qualitative analysis, we show some examples of the predicted segmentation maps from the Pretrained and Adapted models in Figure 2. For each dataset, we show the input images, predictions when all the modalities are available during both training and test time (CMNeXt column), predictions from the pretrained

Table 2: Performance comparison with existing robust methods for MFNet dataset. RGB and Thermal columns report performance when only RGB and Thermal are available. Average column reports average performance when one of the two modalities gets missing. ‘-’ indicates that results for those cells are not published. Mean accuracy (mAcc) and % mean intersection over union (mIoU) are shown for all the experiments.

Methods	RGB		Thermal		Average	
	mAcc	% mIoU	mAcc	% mIoU	mAcc	% mIoU
FuseNet [16]	11.11	10.31	41.33	36.85	26.22	23.58
MFNet [14]	26.62	24.78	19.65	16.64	23.14	20.71
RTFNet [40]	44.89	37.30	26.41	24.57	35.65	30.94
SAGate [6]	32.01	30.57	13.34	12.51	22.68	21.54
FEANet [8]	15.96	8.69	58.35	48.72	37.16	28.71
MDRNet [58]	57.11	45.89	41.98	30.19	49.55	38.04
VPFNet [27]	48.14	41.08	42.20	35.80	45.17	38.44
SpiderMesh [10]	-	39.60	-	50.50	-	45.05
CRM [37]	-	52.70	-	53.10	-	52.90
Adapted (Ours)	67.18	55.22	66.70	50.89	66.94	53.06

Table 3: Performance comparison with existing robust methods for NYUDv2 dataset. RGB and Depth columns report performance when only RGB and Depth are available. Average column indicates average performance when one of the two modalities gets missing. * indicates that available codes and pretrained models from the authors were used to generate the results. Other results are from the corresponding papers.

Methods	RGB		Depth		Average	
	mAcc	% mIoU	mAcc	% mIoU	mAcc	% mIoU
FCN [28]	44.70	31.60	35.70	25.20	40.20	28.40
Dilated FCN-2s [22]	47.10	32.30	39.30	26.80	43.20	29.55
AsymFusion (R-101) [46]	59.00	46.50	45.60	34.30	52.30	40.40
CEN (R-101) [45] *	51.77	39.59	28.98	19.32	40.38	29.46
TokenFusion [44] *	63.49	49.32	46.83	36.84	55.16	43.08
Adapted (Ours)	67.96	52.82	52.42	36.72	60.19	44.77

and adapted models for different available/missing modality scenarios (Available input modality names are shown in parentheses above each image). We see in Figure 2a, the Pretrained model fails to detect humans when only RGB is available and cars when only Thermal images are available. The adapted model can detect both humans and cars with missing modalities. For NYUDv2 dataset, as shown in Figure 2b, the Adapted model can detect window, bed, and furniture with higher accuracy than the Pretrained model with missing modalities. We only show the RGB input images for MCubeS dataset for brevity in Figure 2c. The Adapted model can identify sand, sky, and gravel with higher accuracy than the pretrained model. In all cases, the predictions from the Adapted model with missing modalities are closer to the predictions of the pretrained model with all modalities. We provide additional examples in the supplementary section.

Performance Comparison for RGB-Thermal Semantic Segmentation. We compare the performance of the Adapted model with existing robust models for RGB-thermal semantic segmentation with MFNet dataset in Table 2. The results show that the Adapted model offers the best average performance compared to the other baseline models, in terms of mean accuracy and % mIoU. Among the robust models, CRM [37] shows competitive performance with the Adapted model. The Adapted model performs better when only RGB is available while CRM performs better when only Thermal is available. Notably CRM is designed specifically for RGB-Thermal pairs and requires specialized training approach and utilizes self-distillation loss between the clean and masked modalities to train the model. In contrast, our approach is applicable to any input modalities and does not require any specialized training technique.

Performance Comparison for RGB-Depth Semantic Segmentation. Table 3 shows the performance comparison with existing robust models for RGB-Depth semantic segmentation on NYUDv2 dataset. The table shows that on average, the Adapted model performs better than the existing robust models. TokenFusion [44] performs slightly better (+0.12%) in terms of mIoU when Depth is available and RGB is missing, but shows larger drop (-5.59%) in mean accuracy. On the other hand, the Adapted model performs significantly better (+3.5% mIoU and +4.47% mean accuracy) when RGB is available and Depth is missing. The average performance of the Adapted model is also better than the TokenFusion model despite the fact that TokenFusion was designed to work with RGB-Depth pair, whereas the

Table 4: Performance comparison (% mIoU) of different parameter-efficient adaptation techniques for MFNet, NYUDv2, and MCubeS datasets. Each column reports mIoU of the Adapted model with the corresponding modalities, and Avg indicates average performance. A and D denote Angle and Degree of Linear Polarization.

Datasets	MFNet			NYUDv2			MCubeS			
Methods	RGB	Thermal	Avg	RGB	Depth	Avg	RGB	RGB-A	RGB-A-D	Avg
Pretrained	53.71	35.48	44.60	51.19	5.26	28.23	42.32	48.81	49.06	46.73
Dedicated	55.86	53.34	54.60	52.18	33.49	42.84	48.16	48.42	49.48	48.69
Scale Only	54.77	49.23	52.00	53.04	36.12	44.58	50.16	50.55	51.13	50.61
Shift Only	54.57	48.96	51.77	53.04	36.25	44.65	50.13	50.40	50.86	50.46
BitFit	54.39	49.07	51.73	53.09	36.64	44.87	50.19	50.57	51.07	50.61
LoRA	54.19	47.45	50.82	52.87	34.97	43.92	49.59	50.07	50.80	50.15
Norm	54.65	47.49	51.07	53.05	34.73	43.49	49.95	50.51	51.07	50.51
Scale and Shift	55.22	50.89	53.06	52.82	36.72	44.77	50.43	50.62	51.11	50.72

Table 5: Performance of Pretrained and Adapted models for multimodal sentiment analysis with CMU-MOSI and CMU-MOSEI datasets. Multimodal Transformer (MulT) as the base model. A, V and T denote audio, video, and text, respectively. \uparrow means higher is better and \downarrow means lower is better. The Adapted model outperforms the Pretrained model with missing modalities.

Dataset	Input	Missing	Pretrained			Adapted		
			Acc \uparrow	F1 \uparrow	MAE \downarrow	Acc \uparrow	F1 \uparrow	MAE \downarrow
CMU-MOSI	AVT	-	79.88	79.85	0.918	-	-	-
	AV	T	48.93	41.95	1.961	55.49	53.96	1.469
	A	VT	48.32	40.98	1.875	50.00	46.71	1.464
	V	AT	52.44	51.77	1.547	54.88	54.39	1.471
CMU-MOSEI	AVT	-	83.79	83.75	0.567	-	-	-
	AV	T	41.91	32.78	1.025	63.32	60.69	0.819
	A	VT	37.15	20.12	1.089	62.85	55.55	0.826
	V	AT	38.28	23.70	1.075	62.49	60.00	0.819

Adapted method is independent of input modalities. For our experiments, we use HHA-encoded images proposed by [13] instead of raw depth maps.

Comparison with Parameter Efficient Model Adaption Techniques. Apart from robust models, we also compare different parameter-efficient adaptation techniques. We report the results in Table 4. For MFNet dataset, SSF outperforms all the methods and performance is significantly better than the Pretrained model and close to the Dedicated models. For NYUDv2 and MCubeS datasets, the Adapted model performs better than both Pretrained and Dedicated models. These experiments also show that SSF performs better than other methods for most of the input modality combinations for all the datasets. We show a detailed comparison for each dataset in terms of mean accuracy, F1 score and % mIoU in the supplementary section of this paper.

4.5 Experiments for Multimodal Sentiment Analysis

We tested our adaptation method for a multimodal sentiment analysis task and report the results in Table 5. We used the multimodal transformer (MulT) in [42] as the base model, and the CMU-MOSI dataset in [55] and the CMU-MOSEI dataset in [3] for evaluation. A, V and T stand for audio, video and text modalities, respectively. We observed that when text is available and either audio or video or both are missing at the test time, the performance does not drop significantly. Similar trend was reported in [15]. If text is missing at test time, then the performance of the Pretrained models drops significantly. The Adapted models can partially compensate for missing text and offer significantly better performance.

For CMU-MOSI dataset, we see a significant 30.95% drop in accuracy when text is missing for the pretrained model compared to the case when all modalities are available. The Adapted model offers 6.56% improvement in accuracy over the Pretrained model. We also observe 1.68% and 2.44% improvement in accuracy over the Pretrained model performance when only audio and only video are available, respectively. In all these scenarios, we also see larger improvement in F1 score and reduction in mean absolute error (MAE). For CMU-MOSEI dataset, we see even greater

improvement in all the metrics. Experiments show 21.41%, 25.7% and 24.21% improvement in accuracy for audio-video, audio only, and video only scenarios compared to the Pretrained model. We also observe 27.91%-36.30% improvement in F1 score and 0.206-0.263 reduction in mean absolute error (MAE).

5 Conclusion

Missing modalities at test time can cause significant degradation in the performance of multimodal systems. In this paper, we presented a simple and parameter-efficient adaptation method for robust multimodal learning with missing modalities. We demonstrated that simple linear operations can efficiently transform a single pretrained multimodal network and achieve performance comparable to multiple (independent) dedicated networks trained for different modality combinations. We evaluated the performance of our method and compared with existing robust methods for different multimodal segmentation and sentiment analysis tasks. Our method requires an extremely small number of additional parameters (e.g., $< 0.7\%$ of the total parameters in most experiments), while significantly improving performance compared to missing modality scenarios. Our adaptation strategy is applicable to different network architectures and tasks, which can be a versatile solution to build robust multimodal systems.

Reproducibility Statement

We are committed to ensuring the reproducibility of our research and to facilitate the broader scientific community in replicating and building upon our work. The source code and trained models are available at [github](https://github.com/CSIPlab/Robust-multimodal-learning)¹. We have provided a clear and comprehensive README.md file to guide users in setting up the environment, running the code, and reproducing the results in the paper. We outline the specific data preprocessing steps, list of hyperparameters and configurations used in our experiments in Section 4.2 in the main text and Section B in the supplementary section. We hope this makes it easy for others to replicate our experiments. We have provided scripts and instructions in our source code to reproduce the main experimental results presented in this paper. Additionally, we have provided pretrained models allowing others to directly reproduce the results.

Ethics Statement

To the best of our knowledge this work does not give rise to any significant ethical concerns.

Acknowledgements

This work is supported in part by AFOSR award FA9550-21-1-0330 and NSF CAREER award CCF-2046293.

References

- [1] Jimmy Lei Ba, Jamie Ryan Kiros, and Geoffrey E Hinton. Layer normalization. *Advances in Neural Information Processing Systems: Deep Learning Symposium*. *arXiv preprint arXiv:1607.06450*, 2016.
- [2] Roman Bachmann, David Mizrahi, Andrei Atanov, and Amir Zamir. MultiMAE: Multi-modal multi-task masked autoencoders. In *European Conference on Computer Vision*, 2022.
- [3] AmirAli Bagher Zadeh, Paul Pu Liang, Soujanya Poria, Erik Cambria, and Louis-Philippe Morency. Multimodal language analysis in the wild: CMU-MOSEI dataset and interpretable dynamic fusion graph. In *Proceedings of the 56th Annual Meeting of the Association for Computational Linguistics (Volume 1: Long Papers)*, pages 2236–2246, 2018.
- [4] Tadas Baltrušaitis, Chaitanya Ahuja, and Louis-Philippe Morency. Multimodal machine learning: A survey and taxonomy. *IEEE Transactions on Pattern Analysis and Machine Intelligence*, 41(2):423–443, 2018.
- [5] Elad Ben Zaken, Yoav Goldberg, and Shauli Ravfogel. BitFit: Simple parameter-efficient fine-tuning for transformer-based masked language-models. In *Proceedings of the 60th Annual Meeting of the Association for Computational Linguistics (Volume 2: Short Papers)*, pages 1–9, 2022.

¹<https://github.com/CSIPlab/Robust-multimodal-learning>

- [6] Xiaokang Chen, Kwan-Yee Lin, Jingbo Wang, Wayne Wu, Chen Qian, Hongsheng Li, and Gang Zeng. Bi-directional cross-modality feature propagation with separation-and-aggregation gate for RGB-D semantic segmentation. In *European Conference on Computer Vision (ECCV)*, 2020.
- [7] Jun-Ho Choi and Jong-Seok Lee. EmbraceNet: A robust deep learning architecture for multimodal classification. *Information Fusion*, 51:259–270, 2019.
- [8] Fuqin Deng, Hua Feng, Mingjian Liang, Hongmin Wang, Yong Yang, Yuan Gao, Junfeng Chen, Junjie Hu, Xiyue Guo, and Tin Lun Lam. FEANet: Feature-enhanced attention network for RGB-thermal real-time semantic segmentation. In *2021 IEEE/RSJ International Conference on Intelligent Robots and Systems (IROS)*, pages 4467–4473. IEEE, 2021.
- [9] Reuben Dorent, Samuel Joutard, Marc Modat, Sébastien Ourselin, and Tom Vercauteren. Hetero-modal variational encoder-decoder for joint modality completion and segmentation. In *Medical Image Computing and Computer Assisted Intervention–MICCAI 2019: 22nd International Conference, Shenzhen, China, October 13–17, 2019, Proceedings, Part II* 22, pages 74–82. Springer, 2019.
- [10] Siqi Fan, Zhe Wang, Yan Wang, and Jingjing Liu. SpiderMesh: Spatial-aware demand-guided recursive meshing for RGB-T semantic segmentation. *arXiv:2303.08692*, 2023.
- [11] Ahmed Gomaa, Andreas Maier, and Ronak Kosti. Supervised contrastive learning for robust and efficient multimodal emotion and sentiment analysis. In *2022 26th International Conference on Pattern Recognition (ICPR)*, pages 2423–2429. IEEE, 2022.
- [12] Matthieu Guillaumin, Jakob Verbeek, and Cordelia Schmid. Multimodal semi-supervised learning for image classification. In *2010 IEEE Computer Society Conference on Computer Vision and Pattern Recognition*, pages 902–909. IEEE, 2010.
- [13] Saurabh Gupta, Ross Girshick, Pablo Arbeláez, and Jitendra Malik. Learning rich features from RGB-D images for object detection and segmentation. In *European Conference on Computer Vision*, pages 345–360, 2014.
- [14] Qishen Ha, Kohei Watanabe, Takumi Karasawa, Yoshitaka Ushiku, and Tatsuya Harada. MFNet: Towards real-time semantic segmentation for autonomous vehicles with multi-spectral scenes. In *2017 IEEE/RSJ International Conference on Intelligent Robots and Systems (IROS)*, pages 5108–5115, 2017.
- [15] Devamanyu Hazarika, Yingting Li, Bo Cheng, Shuai Zhao, Roger Zimmermann, and Soujanya Poria. Analyzing modality robustness in multimodal sentiment analysis. In *Proceedings of the 2022 Conference of the North American Chapter of the Association for Computational Linguistics: Human Language Technologies*, pages 685–696, Seattle, United States, July 2022. Association for Computational Linguistics.
- [16] Caner Hazirbas, Lingni Ma, Csaba Domokos, and Daniel Cremers. FuseNet: Incorporating depth into semantic segmentation via fusion-based CNN architecture. In *Asian Conference on Computer Vision*, 2016.
- [17] Kaiming He, Xinlei Chen, Saining Xie, Yanghao Li, Piotr Dollár, and Ross Girshick. Masked autoencoders are scalable vision learners. In *Proceedings of the IEEE/CVF Conference on Computer Vision and Pattern Recognition*, pages 16000–16009, 2022.
- [18] Xuehai He, Chunyuan Li, Pengchuan Zhang, Jianwei Yang, and Xin Eric Wang. Parameter-efficient model adaptation for vision transformers. *Proceedings of the AAAI Conference on Artificial Intelligence*, 37(1):817–825, Jun. 2023.
- [19] Edward J Hu, Yelong Shen, Phillip Wallis, Zeyuan Allen-Zhu, Yanzhi Li, Shean Wang, Lu Wang, and Weizhu Chen. LoRA: Low-rank adaptation of large language models. In *International Conference on Learning Representations*, 2022.
- [20] Ahmed Hussen Abdelaziz, Barry-John Theobald, Paul Dixon, Reinhard Knothe, Nicholas Apostoloff, and Sachin Kajareker. Modality dropout for improved performance-driven talking faces. In *Proceedings of the 2020 International Conference on Multimodal Interaction*, pages 378–386, 2020.
- [21] Sergey Ioffe and Christian Szegedy. Batch normalization: Accelerating deep network training by reducing internal covariate shift. In *International Conference on Machine Learning*, pages 448–456, 2015.
- [22] Sharif Amit Kamran and Ali Shihab Sabbir. Efficient yet deep convolutional neural networks for semantic segmentation. In *2018 International Symposium on Advanced Intelligent Informatics (SAIN)*, pages 123–130, 2018.
- [23] Ramandeep Kaur and Sandeep Kautish. Multimodal sentiment analysis: A survey and comparison. *Research Anthology on Implementing Sentiment Analysis Across Multiple Disciplines*, pages 1846–1870, 2022.
- [24] Kenneth Lau, Jonas Adler, and Jens Sjölund. A unified representation network for segmentation with missing modalities. *arXiv preprint arXiv:1908.06683*, 2019.

- [25] Dongze Lian, Daquan Zhou, Jiashi Feng, and Xinchao Wang. Scaling & shifting your features: A new baseline for efficient model tuning. In *Advances in Neural Information Processing Systems (NeurIPS)*, 2022.
- [26] Yupeng Liang, Ryosuke Wakaki, Shohei Nobuhara, and Ko Nishino. Multimodal material segmentation. In *Proceedings of the IEEE/CVF Conference on Computer Vision and Pattern Recognition (CVPR)*, pages 19800–19808, June 2022.
- [27] Baihong Lin, Zengrong Lin, Yulan Guo, Yulan Zhang, Jianxiao Zou, and Shicai Fan. Variational probabilistic fusion network for RGB-T semantic segmentation. *arXiv preprint arXiv:2307.08536*, 2023.
- [28] Jonathan Long, Evan Shelhamer, and Trevor Darrell. Fully convolutional networks for semantic segmentation. In *2015 IEEE Conference on Computer Vision and Pattern Recognition (CVPR)*, pages 3431–3440, 2015.
- [29] Ilya Loshchilov and Frank Hutter. Decoupled weight decay regularization. In *International Conference on Learning Representations*, 2019.
- [30] Mengmeng Ma, Jian Ren, Long Zhao, Davide Testuggine, and Xi Peng. Are multimodal transformers robust to missing modality? In *Proceedings of the IEEE/CVF Conference on Computer Vision and Pattern Recognition*, pages 18177–18186, 2022.
- [31] Harsh Maheshwari, Yen-Cheng Liu, and Zsolt Kira. Missing modality robustness in semi-supervised multi-modal semantic segmentation. *arXiv preprint arXiv:2304.10756*, 2023.
- [32] Brandon McKinzie, Joseph Cheng, Vaishaal Shankar, Yinfei Yang, Jonathon Shlens, and Alexander Toshev. On robustness in multimodal learning. *arXiv preprint arXiv:2304.04385*, 2023.
- [33] Natalia Neverova, Christian Wolf, Graham Taylor, and Florian Nebout. ModDrop: Adaptive multi-modal gesture recognition. *IEEE Transactions on Pattern Analysis and Machine Intelligence*, 38(8):1692–1706, 2015.
- [34] Giulia Rizzoli, Francesco Barbato, and Pietro Zanuttigh. Multimodal semantic segmentation in autonomous driving: A review of current approaches and future perspectives. *Technologies*, 10(4):90, 2022.
- [35] Swalpa Kumar Roy, Ankur Deria, Danfeng Hong, Behnood Rasti, Antonio Plaza, and Jocelyn Chanussot. Multimodal fusion transformer for remote sensing image classification. *IEEE Transactions on Geoscience and Remote Sensing*, 2023.
- [36] Anmol Sharma and Ghassan Hamarneh. Missing MRI pulse sequence synthesis using multi-modal generative adversarial network. *IEEE Transactions on Medical Imaging*, 39(4):1170–1183, 2019.
- [37] Ukcheol Shin, Kyunghyun Lee, and In So Kweon. Complementary random masking for RGB-Thermal semantic segmentation. *arXiv preprint arXiv:2303.17386*, 2023.
- [38] Nathan Silberman, Derek Hoiem, Pushmeet Kohli, and Rob Fergus. Indoor segmentation and support inference from RGBD images. In *European Conference on Computer Vision*, 2012.
- [39] Mohammad Soleymani, David Garcia, Brendan Jou, Björn Schuller, Shih-Fu Chang, and Maja Pantic. A survey of multimodal sentiment analysis. *Image and Vision Computing*, 65:3–14, 2017.
- [40] Yuxiang Sun, Weixun Zuo, and Ming Liu. RTFNet: RGB-Thermal Fusion Network for Semantic Segmentation of Urban Scenes. *IEEE Robotics and Automation Letters*, 4(3):2576–2583, July 2019.
- [41] Antti Tarvainen and Harri Valpola. Mean teachers are better role models: Weight-averaged consistency targets improve semi-supervised deep learning results. *Advances in Neural Information Processing Systems*, 30, 2017.
- [42] Yao-Hung Hubert Tsai, Shaojie Bai, Paul Pu Liang, J. Zico Kolter, Louis-Philippe Morency, and Ruslan Salakhutdinov. Multimodal transformer for unaligned multimodal language sequences. In *Proceedings of the 57th Annual Meeting of the Association for Computational Linguistics*, pages 6558–6569, Florence, Italy, July 2019. Association for Computational Linguistics.
- [43] Hu Wang, Yuanhong Chen, Congbo Ma, Jodie Avery, Louise Hull, and Gustavo Carneiro. Multi-modal learning with missing modality via shared-specific feature modelling. In *Proceedings of the IEEE/CVF Conference on Computer Vision and Pattern Recognition*, pages 15878–15887, 2023.
- [44] Yikai Wang, Xinghao Chen, Lele Cao, Wenbing Huang, Fuchun Sun, and Yunhe Wang. Multimodal token fusion for vision transformers. In *IEEE Conference on Computer Vision and Pattern Recognition (CVPR)*, 2022.
- [45] Yikai Wang, Wenbing Huang, Fuchun Sun, Tingyang Xu, Yu Rong, and Junzhou Huang. Deep multimodal fusion by channel exchanging. In *Advances in Neural Information Processing Systems (NeurIPS)*, 2020.
- [46] Yikai Wang, Fuchun Sun, Ming Lu, and Anbang Yao. Learning deep multimodal feature representation with asymmetric multi-layer fusion. In *ACM International Conference on Multimedia (ACM MM)*, 2020.

- [47] Sangmin Woo, Sumin Lee, Yeonju Park, Muhammad Adi Nugroho, and Changick Kim. Towards good practices for missing modality robust action recognition. In *Proceedings of the AAAI Conference on Artificial Intelligence*, volume 37, 2023.
- [48] Mitchell Wortsman, Gabriel Ilharco, Jong Wook Kim, Mike Li, Simon Kornblith, Rebecca Roelofs, Raphael Gontijo Lopes, Hannaneh Hajishirzi, Ali Farhadi, and Hongseok Namkoong. Robust fine-tuning of zero-shot models. In *Proceedings of the IEEE/CVF Conference on Computer Vision and Pattern Recognition*, pages 7959–7971, 2022.
- [49] Yi Xiao, Felipe Codevilla, Akhil Gurram, Onay Urfalioglu, and Antonio M López. Multimodal end-to-end autonomous driving. *IEEE Transactions on Intelligent Transportation Systems*, 23(1):537–547, 2020.
- [50] Enze Xie, Wenhai Wang, Zhiding Yu, Anima Anandkumar, Jose M Alvarez, and Ping Luo. SegFormer: Simple and efficient design for semantic segmentation with transformers. In *Neural Information Processing Systems (NeurIPS)*, 2021.
- [51] Peng Xu, Xiatian Zhu, and David A Clifton. Multimodal learning with transformers: A survey. *IEEE Transactions on Pattern Analysis and Machine Intelligence*, 2023.
- [52] Biting Yu, Luping Zhou, Lei Wang, Jurgen Fripp, and Pierrick Bourgeat. 3D cGAN based cross-modality MR image synthesis for brain tumor segmentation. In *2018 IEEE 15th International Symposium on Biomedical Imaging (ISBI 2018)*, pages 626–630. IEEE, 2018.
- [53] Jun Yu, Jing Li, Zhou Yu, and Qingming Huang. Multimodal transformer with multi-view visual representation for image captioning. *IEEE Transactions on Circuits and Systems for Video Technology*, 30(12):4467–4480, 2019.
- [54] Wenmeng Yu, Hua Xu, Ziqi Yuan, and Jiele Wu. Learning modality-specific representations with self-supervised multi-task learning for multimodal sentiment analysis. In *Proceedings of the AAAI Conference on Artificial Intelligence*, volume 35, pages 10790–10797, 2021.
- [55] Amir Zadeh, Rowan Zellers, Eli Pincus, and Louis-Philippe Morency. Multimodal sentiment intensity analysis in videos: Facial gestures and verbal messages. *IEEE Intelligent Systems*, 31(6):82–88, 2016.
- [56] Jiaming Zhang, Ruiping Liu, Hao Shi, Kailun Yang, Simon Reiß, Kunyu Peng, Haodong Fu, Kaiwei Wang, and Rainer Stiefelhagen. Delivering arbitrary-modal semantic segmentation. In *Proceedings of the IEEE/CVF Conference on Computer Vision and Pattern Recognition*, pages 1136–1147, 2023.
- [57] Dexin Zhao, Zhi Chang, and Shutao Guo. A multimodal fusion approach for image captioning. *Neurocomputing*, 329:476–485, 2019.
- [58] Shenlu Zhao, Yichen Liu, Qiang Jiao, Qiang Zhang, and Jungong Han. Mitigating modality discrepancies for RGB-T semantic segmentation. *IEEE Transactions on Neural Networks and Learning Systems*, pages 1–15, 2023.

SUPPLEMENTARY MATERIAL

A Datasets

MFNet Dataset introduced by [14], is a popular dataset for RGB-thermal urban scene segmentation, particularly in the context of supporting autonomous driving applications. It comprises a total of 1569 aligned pairs of RGB-thermal images. Within this collection, 820 image pairs were captured during daytime, while 749 pairs were acquired during nighttime. The dataset is divided into distinct training and test sets, each accompanied by pixel-level annotations that define semantic labels for nine classes. Each image is 640×480 pixels.

NYU Depth v2 (NYUDv2) Dataset from [38] is a well-known dataset for RGB-D semantic segmentation. This dataset contains 1449 pairs of aligned RGB-depth images of indoor scenes. The images are divided into training and test sets containing 795 and 654 pairs of images respectively. The dataset also provides per pixel annotations for 13 classes, 40 classes and 894 classes ground truth semantic labels. For our experiments we used the standard 40 classes annotation. Each image is 640×480 pixels and the dataset contains both raw and processed depth maps. For our experiments we used HHA images as proposed by [13] instead of depth maps.

Multimodal Material Segmentation (MCubeS) Dataset was introduced by [26] for accurate multimodal material segmentation with the help of thermal and polarized images alongside RGB images. This dataset has four modalities: RGB, Angle of Linear Polarization, Degree of Linear Polarization and Near-Infrared. Alongside these modalities, the dataset also provides ground truth annotation for semantic and material segmentation. There are 500 image sets divided into train, validation and test sets having 302, 96 and 102 image sets respectively. The images are 1224×1024 pixels each and have 20 classes in total.

CMU-MOSI dataset from [55] is a popularly used for multimodal sentiment analysis. The dataset has 2199 samples each having audio, visual and text as input modalities. It is divided into train, validation and test sets containing 1284, 229 and 686 samples respectively along with annotated sentiment for each sample.

CMU-MOSEI is a large scale sentiment analysis dataset from [3]. It is 10 times larger than CMU-MOSI and contains audio, visual and text modalities along with ground truth sentiment annotations. The dataset contains 23453 samples divided into train, validation and test sets for multimodal sentiment analysis and emotion recognition.

B Implementation Details

We used Python² 3.8.12 and PyTorch³ 1.9.0 to for our implementation. The experiments were done using two NVIDIA RTX 2080 Ti GPUs. We applied automatic mixed precision (AMP) training provided by PyTorch. For CMNeXt model, we use their publicly available code⁴ and models trained on all the available modalities for each dataset. We trained the multimodal transformer models on all the modalities using the available code and preprocessed data from the repository⁵ for CMU-MOSI and CMU-MOSEI datasets.

MFNet Dataset: We divided the 4 channel RGB-T images into three channel RGB and one channel thermal images. Then data pre-processing and augmentation was applied following CMNeXt from [56]. MiT-B4 from [50] was the backbone for the base CMNeXt model. One set of scale and shift parameters was learnt for each input modality combination. Input images were sized at 640×480 for both training and testing and we report single scale performance for all the experiments. The scale and shift parameters were trained for 100 epochs with a batch size of 4.

NYUDv2 Dataset: For processing depth maps, we follow SA-Gate by [6] and CMNeXt by [56] and use HHA-encoded images instead of raw depth maps. The already preprocessed dataset can be downloaded from the SA-Gate repository⁶. RGB and HHA images were sized at 640×480 pixels each and we used this size for training and testing. The backbone was set to MiT-B4 as suggested in CMNeXt paper. One set of scale and shift parameters was learnt for each input modality combination by feeding available input modalities and setting the missing modality to zero. We train the scale and shift parameters for 100 epochs with a batch size of 4 and report single scale performance.

MCubeS Dataset: We follow the same data pre-processing and augmentations used by the base CMNeXt model from [56]. MiT-B2 from [50] was used as the backbone for this dataset. We set the input image resolution to 512×512 during training and 1024×1024 during testing and report single scale performance with predicted segmentation maps

²<https://www.python.org/>

³<https://pytorch.org/>

⁴<https://github.com/jamyeung/DELIVER>

⁵<https://github.com/thuiar/MMSA>

⁶https://github.com/charlesCXX/RGBD_Semantic_Segmentation_PyTorch

Table 6: Hyperparameters for the experiments on CMU-MOSI and CMU-MOSEI datasets for multimodal sentiment analysis.

Hyperparameters	CMU-MOSI	CMU-MOSEI
Batch Size	16	4
Initial Learning Rate	0.002	0.0005
Optimizer	Adam	Adam
Attention Dropout	0.3	0.4
Embedding Dropout	0.2	0.0
Output Dropout	0.5	0.5
Gradient Clip	0.6	0.6
Weight Decay	0.005	0.001
Temporal Conv Kernel Size (T/A/V)	5/5/5	5/1/3
# of Crossmodal Blocks	4	4

Table 7: Learnable parameter counts for different parameter efficient model adaptation methods. As seen from the table, scale and shift introduce less than 0.7% of the total model parameters.

Method	Total Parameters (M)	Learnable Parameters (M)	% of Total Parameters
Norm	116.560	0.126	0.108
BitFit	116.560	0.378	0.324
LoRA	116.957	0.397	0.340
Scale and Shift	117.349	0.789	0.673

sized at 1024×1024 . Similar to other two datasets, we train the learnable parameters for 100 epochs with a batch size of 4.

CMU-MOSI and CMU-MOSEI Datasets: We used Multimodal Transformer (MulT) from [42] as the base model. Preprocessed datasets and all the configurations are available on the repository⁷. First we trained the multimodal transformer (MulT) model on all the available modalities and then adapted the pretrained model for different modalities. The hyperparameters for the experiments are shown in Table 6.

C Number of Learnable Parameters

We report the number of learnable parameters for different parameter-efficient adaptation techniques (for multimodal segmentation) in Table 7. We insert scale and shift layers after each linear, convolutional and norm (both batch norm and layer norm) layers. The number of learnable parameter varies with the size of the backbone. We used MiT-B4 as the backbone while counting these learnable parameters. Scale and shift adds only 0.789M learnable parameters which is less than 0.7% of the total model parameters. Despite this very few parameters, it improves performance significantly in different missing modality scenarios. For this study we mainly focused on improving missing modality robustness and did not try to optimize the number of learnable parameters. We will leave that part for future studies.

D Comparison of Parameter-Efficient Adaptation Methods

We performed a detailed performance comparison with other parameter efficient methods for the three segmentation datasets. The results are summarized in Table 8 for RGB-thermal segmentation on MFNet dataset, Table 9 for RGB-depth segmentation on NYUDv2 dataset and Table 10 for multimodal material segmentation on MCubeS dataset. For each method, we take a model trained on all the available modalities. Then we freeze the pretrained weights and tune the learnable parameters for the corresponding adaption method. We have shown mean accuracy, F1 score and % mIoU for each experiment.

D.1 Comparison for RGB-Thermal Semantic Segmentation

Table 8 summarizes the results on MFNet dataset when the base CMNeXt model is adapted with other parameter efficient model adaptation techniques. Experiments show that scale and shift shows the best performance in all three

⁷<https://github.com/thuiar/MMSA>

Table 8: Performance comparison with parameter efficient model adaptation techniques on CMNeXt model for MFNet dataset. Average column indicates average performance when one of the two modalities gets missing. Mean accuracy, F1 score and % mIoU are shown for all the experiments.

Methods	RGB			Thermal			Average		
	mAcc	F1	% mIoU	mAcc	F1	% mIoU	mAcc	F1	% mIoU
Pretrained	60.74	66.91	53.71	38.18	45.11	35.48	49.46	56.01	44.60
Dedicated	66.28	68.22	55.86	68.35	65.29	53.34	67.32	66.76	54.60
Scale Only	67.09	68.03	54.77	64.00	60.92	49.23	65.55	64.48	52.00
Shift Only	65.82	67.42	54.57	59.77	60.54	48.96	62.80	63.98	51.77
BitFit	66.49	67.40	54.39	61.06	60.59	49.07	63.78	64.00	51.73
LoRA	66.44	67.32	54.19	57.10	59.04	47.45	61.77	63.18	50.82
Norm	66.43	67.07	54.65	57.55	59.22	47.49	61.99	63.15	51.07
Scale and Shift	67.18	68.04	55.22	66.70	62.64	50.89	66.94	65.34	53.06

Table 9: Performance comparison with parameter efficient model adaptation techniques on CMNeXt model for NYUDv2 dataset. Average column indicates average performance when one of the two modalities gets missing. Mean accuracy, F1 score and % mIoU are shown for all the experiments.

Methods	RGB			Depth			Average		
	mAcc	F1	% mIoU	mAcc	F1	% mIoU	mAcc	F1	% mIoU
Pretrained	64.10	65.70	51.19	8.30	7.95	5.26	36.20	36.83	28.23
Dedicated	66.00	66.62	52.18	44.80	46.79	33.49	55.40	56.71	42.84
Scale Only	68.18	67.38	53.04	51.54	49.88	36.12	59.86	58.63	44.58
Shift Only	67.54	67.35	53.04	50.30	49.76	36.25	58.92	58.56	44.65
BitFit	67.31	67.33	53.09	50.68	50.27	36.64	59.00	58.80	44.87
LoRA	66.67	67.14	52.87	49.34	48.66	34.97	58.01	57.90	43.92
Norm	67.18	67.34	53.05	48.74	48.06	34.73	57.96	57.70	43.89
Scale and Shift	67.96	67.18	52.82	52.42	50.60	36.72	60.19	58.89	44.77

matrices compared to all other methods. It shows a significant improvement of +8.46% in mIoU, +9.33% in F1 score and +17.48% in mean accuracy on an average over the pretrained model. The average performance is also close to dedicatedly trained models.

D.2 Comparison for RGB-Depth Semantic Segmentation

Similar trend is observed for RGB-depth semantic segmentation on NYUDv2 dataset as shown in Table 9. Scale only and BitFit adapted models show slightly better performance for some of the matrices. But in most of the cases scale and shift adapted model performs better. For all the matrices, scale and shift shows a significant improvement of +16.54% in mIoU, +22.05% in F1 score and +23.99% in mean accuracy over the pretrained model on an average and consistently outperforms dedicated training.

D.3 Comparison for Multimodal Material Segmentation

We show comparison with parameter efficient model adaptation techniques on MCubeS dataset in Table 10. Scale and shift outperforms all other methods in most of the matrices for all input combinations. It also shows an improvement of +3.99% in mIoU, +3.57% in F1 score and +3.74% in mean accuracy on an average over the pretrained model. Furthermore, Scale and shift also outperforms dedicated training for all input modality combinations. These experiments corroborate the fact that scale and shift provides better model adaption for different missing modality scenarios.

E Per Class IoU Comparison

To further analyze how the adaption is helping the model improve overall semantic and material segmentation performance, we conduct a per-class % intersection over union (IoU) analysis on the pretrained and adapted models. Table 11 summarizes the results. We show the per class % IoU comparison for different missing modality situations

Table 10: Performance comparison with different parameter efficient model adaptation techniques on CMNeXt model for MCubeS dataset. Average column indicates the average performance. Mean accuracy, F1 score and % mIoU are shown for all the experiments.

Methods	RGB			RGB-AoLP			RGB-AoLP-DoLP			Average		
	mAcc	F1	% mIoU	mAcc	F1	% mIoU	mAcc	F1	% mIoU	mAcc	F1	% mIoU
Pretrained	51.63	55.91	42.32	58.66	62.00	48.81	60.06	62.43	49.06	56.78	60.11	46.73
Dedicated	57.70	60.95	48.16	57.56	61.17	48.42	59.12	61.91	49.48	58.13	61.34	48.69
Scale Only	59.64	63.06	50.16	60.28	63.55	50.55	60.96	64.14	51.13	60.29	63.58	50.61
Shift Only	59.82	63.17	50.13	60.10	63.36	50.40	60.61	63.78	50.86	60.18	63.44	50.46
BitFit	59.98	63.24	50.19	60.12	63.52	50.57	60.84	64.03	51.07	60.31	63.60	50.61
LoRA	59.08	62.50	49.59	59.81	63.05	50.07	60.69	63.84	50.80	59.86	63.13	50.15
Norm	59.57	62.89	49.95	60.22	63.49	50.51	60.98	64.08	51.07	60.26	63.49	50.51
Scale and Shift	60.23	63.41	50.43	60.40	63.59	50.62	60.94	64.04	51.11	60.52	63.68	50.72

on MFNet dataset on Table 11a. From the table we can see that when RGB is available and thermal is missing, the adaptation helps improve performance for most of the classes. Though we see some performance drop for bike (-0.74%) and guardrail (-5.25%) classes, the rest of the classes have better % IoU than the pretrained model. Bump (+6.26%), person (+4.42%), and curve (+4.14%) classes show greater improvement after adaptation. When thermal is available and RGB is missing, adaptation improves performance for all the classes. Among the classes, bike (+39.76%), car (+27.59%), car stop (+24.04%), color cone (+19.37%) and bump (+13.91%) are showing impressive performance improvement over the pretrained model.

Results for MCubeS dataset is shown on Table 11b. Here A, D, and N stand for angle of linear polarization (AoLP), degree of linear polarization (DoLP) and near-infrared (NIR) respectively. Experiments show that when only RGB is available and the rest of the modalities are missing, the adapted model performs better in detecting all the 20 classes present in the dataset. Gravel (36.2%), asphalt (16.1%), rubber (15.2%), wood (12.9%) and sky (10.2%) are some of the classes who show the most performance boost after adaptation. In other input combinations, most of the classes see performance improvement compared to the pretrained model. Though we see some performance drop in a few classes, most of the classes show improvement in % IoU which leads to the overall performance improvement after adaption.

F Examples of Predicted Segmentation Maps

We show the predicted segmentation maps from the pretrained and adapted models in Figure 3. For each dataset, we show the input images, predictions from the base CMNeXt model when all the modalities are available, predictions from the adapted and pretrained models for different missing modality scenarios. For brevity, we only show RGB input images for MCubeS dataset. A, D and N stand for angle of linear polarization (AoLP), degree of linear polarization (DoLP) and near-infrared (NIR) respectively. Modalities that are available during testing are shown in parenthesis while other modalities are missing.

For MFNet dataset, Figure 3a shows that when only RGB is available, the pretrained model performs very poorly in detecting humans. On the other hand, if only thermal is available, the pretrained model can not detect cars very accurately. But the adapted model can detect both humans and cars more accurately in both of the scenarios. In all the cases, the predictions from the adapted model is closer to the predictions of the base CMNeXt model when all the modalities are available.

Predictions from NYUDv2 dataset is shown on Figure 3b. We can see that the adapted model can identify bed, furniture and other classes more accurately than the pretrained model for different missing modality scenarios. The pretrained model performs very poorly when only depth is available and RGB is missing. But detection accuracy improves significantly after model adaptation. For MCubeS dataset, as seen in Figure 3c, predictions from the pretrained model shows artifacts when detecting different materials. On the other hand, the adapted model is showing more accuracy in detecting sky, cobblestone, sand and brick. For all the three datasets, the predictions from the adapted model is more accurate and closer to the all modality predictions of the base CMNeXt model.

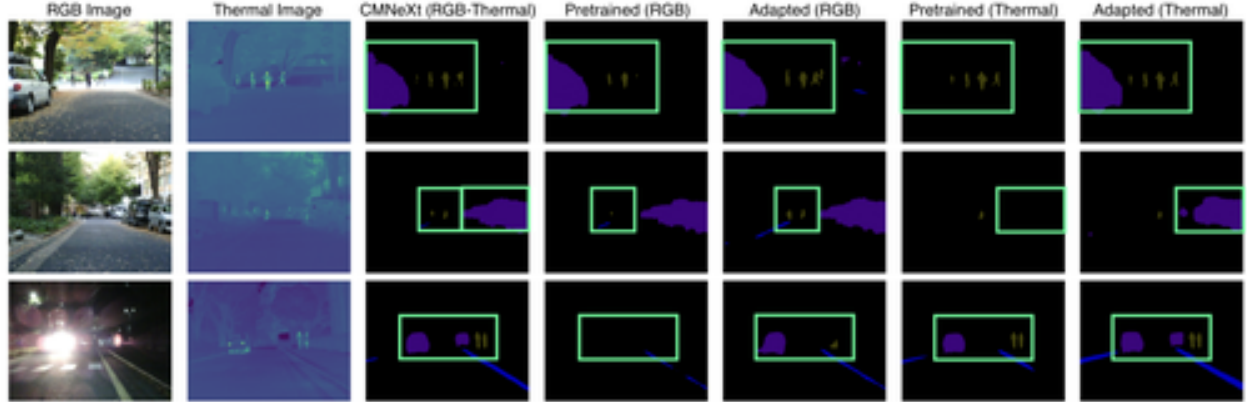
Table 11: Per class % IoU comparison between pretrained and adapted CMNeXt model on MFNet and MCubeS datasets. Adapted model show better performance for most of the classes leading to overall performance improvement. Here A, D and N stand for Angle of Linear Polarization (AoLP), Degree of Linear Polarization (DoLP) and Near-Infrared (NIR) respectively.

(a) Per class % IoU of pretrained and adapted CMNeXt model on MFNet dataset.

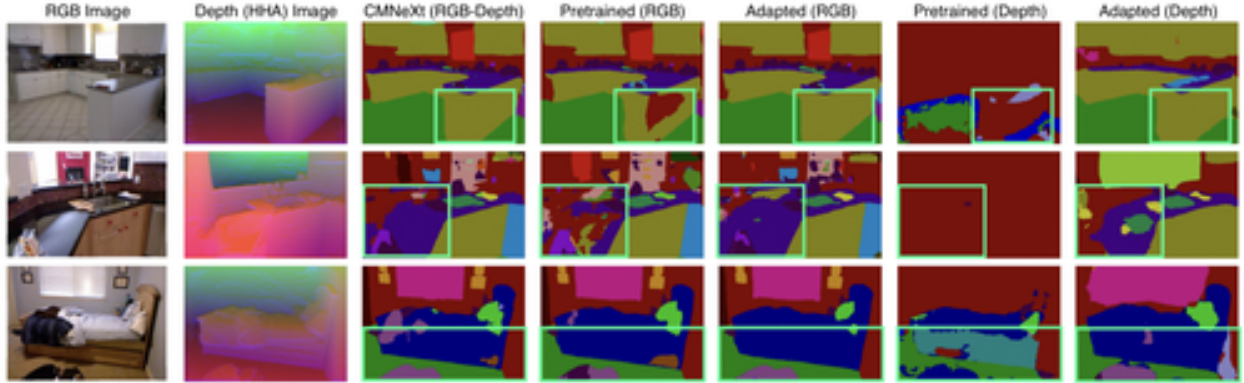
Modalities	Methods	Unlabeled	Car	Person	Bike	Curve	Car_Stop	Guardrail	Color_Cone	Bump	Mean
RGB-Thermal	CMNeXt	98.31	90.27	74.52	64.52	46.64	39.19	15.09	52.56	59.79	60.10
RGB	Pretrained	97.79	87.62	51.13	61.94	30.05	39.36	21.04	45.55	48.95	53.71
	Adapted	97.79	88.06	55.55	61.20	34.19	40.52	15.78	48.67	55.21	55.22
Thermal	Pretrained	95.97	55.24	68.47	9.27	31.85	2.75	0.0	16.87	38.92	35.48
	Adapted	97.46	82.83	70.12	49.03	40.89	26.79	1.84	36.24	52.83	50.89

(b) Per class % IoU of pretrained and adapted CMNeXt model on MCubeS dataset.

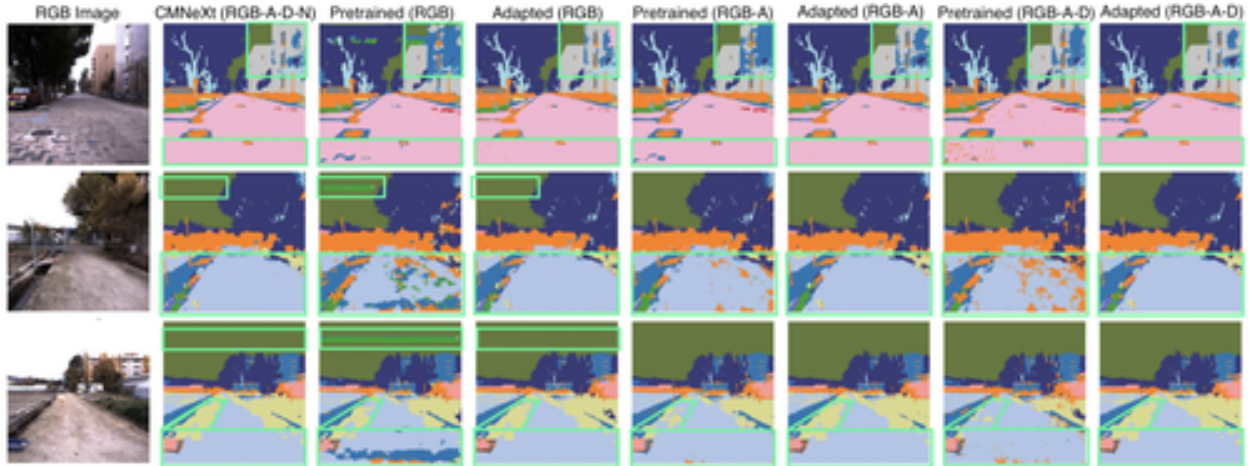
Modalities	Methods	Asphalt	Concrete	Metal	Road_Marking	Fabric	Glass	Plaster	Plastic	Rubber	Sand	Gravel	Ceramic	Cobblestone	Brick	Grass	Wood	Leaf	Water	Human	Sky	Mean
RGB-A-D-N	CMNeXt	84.4	44.9	53.9	74.6	32.1	54.0	0.8	28.7	29.8	67.0	66.2	27.7	68.5	42.8	58.7	49.7	75.3	55.6	19.1	96.52	51.5
RGB	Pretrained	69.7	39.2	47.6	67.3	26.9	44.6	0.2	20.9	15.2	61.8	36.7	19.1	67.2	36.0	49.5	36.1	71.6	36.1	14.7	86.3	42.3
	Adapted	85.8	43.7	52.6	73.8	27.9	51.0	0.8	24.2	30.4	67.8	72.9	27.1	68.1	42.9	57.6	49.0	74.9	43.4	18.3	96.5	50.4
RGB-A	Pretrained	83.2	43.3	50.7	72.6	26.4	51.9	0.2	28.1	22.2	67.7	63.4	22.7	67.5	40.6	54.4	44.9	73.9	44.8	21.8	96.0	48.8
	Adapted	84.4	45.4	53.8	74.5	30.4	53.2	0.6	26.9	28.8	69.0	69.3	24.8	67.5	43.2	58.4	48.2	75.1	48.1	14.4	96.4	50.6
RGB-A-D	Pretrained	84.5	41.2	46.7	72.8	25.2	51.6	0.3	26.1	28.8	66.7	65.6	26.0	66.5	40.4	50.0	45.1	72.7	49.4	25.6	96.3	49.1
	Adapted	84.1	45.6	54.1	74.6	30.5	54.2	0.6	28.1	30.1	69.0	67.6	25.9	67.8	43.8	58.0	49.1	75.0	53.7	13.7	96.5	51.1



(a) Visualization of predictions from MFNet dataset



(b) Visualization of predictions from NYUDv2 dataset



(c) Visualization of predictions from MCubeS dataset

Figure 3: Visualization of predicted segmentation maps for pretrained and adapted models on MFNet and NYUDv2 datasets for multimodal semantic segmentation and MCubeS dataset for multimodal material segmentation. Only RGB images are shown from MCubeS dataset for brevity. CMNeXt column shows the predictions when all the modalities are available. Segmentation quality improves significantly after model adaptation for all the input modality combinations. A, D and N stand for angle of linear polarization, degree of linear polarization and near-infrared respectively.